Genetic Optimization for the Design of a Machine Tool Slide Table for Reduced Energy Consumption

Matthew J. Triebe[1]
Environmental and Ecological Engineering,
Purdue University,
500 Central Drive,
West Lafayette, IN 47907
e-mail: mtriebe@purdue.edu

Fu Zhao
Environmental and Ecological Engineering,
School of Mechanical Engineering,
Purdue University,
585 Purdue Mall,
West Lafayette, IN 47907
e-mail: fzhao@purdue.edu

John W. Sutherland
Environmental and Ecological Engineering,
Purdue University,
500 Central Drive,
West Lafayette, IN 47907
e-mail: jwsuther@purdue.edu

Reducing the energy consumption of machine tools is important from a sustainable manufacturing perspective. Much of a machine tool's environmental impact comes from the energy it consumes during its use phase. To move elements of a machine tool requires energy, and if the mass of those elements can be reduced, then the required energy would be reduced. Therefore, this paper proposes a genetic algorithm to design lightweight machine tools to reduce their energy consumption. This is specifically applied to optimize the structure of a machine tool slide table, which moves throughout the use of the machine tool, with the goal of reducing its mass without sacrificing its stiffness. The table is envisioned as a sandwich panel, and the proposed genetic algorithm optimizes the core of the sandwich structure while considering both mass and stiffness. A finite element model is used to assess the strength of the proposed designs. Finite element results indicate that the strength of the lightweight tables is comparable with a traditional table design. [DOI: 10.1115/1.4050551]

Keyword: sustainable manufacturing

1 Introduction

Manufacturing plays a vital role in our lives. It provides the goods needed by consumers and industries worldwide for global development and for improving the quality of life. It contributes to wealth generation and job creation. In 2017, 30% of the global gross domestic product (GDP) was attributed to industry [1], and manufacturing represents the largest portion of industrial activities. Further, manufacturing supplies employment for nearly 25% of the global labor force of 3.43 billion people [1].

However, along with its benefits, manufacturing does create an environmental burden through non-renewable resources and energy consumption/depletion, and waste streams. For example, in 2020 among all end users, industry accounted for 26.4% of the energy consumption in the US [2], with much of the electricity being generated from fossil fuels [3,4]. Without action, the environmental burden of manufacturing is expected to grow unabated as the world population and standard of living continue to increase.

One major class of equipment used to manufacture components are machine tools (MTs), and MT sales in 2018 were $144.6 billion with projected sales in 2023 of $174 billion [5]. MTs, e.g., lathes, milling machines, and drill presses, are often used to undertake machining operations, and when MTs perform these operations, they consume large amounts of energy and create a substantial environmental impact. Like any product, an MT has a lifecycle: extraction of resources, materials processing, manufacturing, and assembly of components to create the MT, use, and end-of-life. The longest lifecycle stage for an MT is its use stage, and because of conspicuous electricity consumption during its use, which can be up to 80% [6] of the energy consumed throughout its lifecycle, the use stage is the most dominant in terms of carbon footprint and environmental impact [6,7]. This is the case since electricity used by MTs is largely generated from fossil fuels, especially in the US with over 80% produced from fossil fuels [3,4].

One potential approach falling under the structural optimization category for reducing the energy consumed during the use stage of an MT is lightweighting (LW) [8,9]. As is the case for automobiles [10], the greater the MT mass the more energy is required, especially for MT elements that move during the use of the MT. Kroll et al. [8] explored the potential of LW to reduce an MT's energy consumption along with other benefits such as increased acceleration capability and process stability. Hermann et al. [9] further examined LW potential by showing how the reduction in energy consumption during the use stage as a result of LW can offset any potential impacts during other lifecycle stages. To effectively reduce energy consumption through LW, it must be implemented through design, which as noted by Yoon et al. [11], has the greatest potential for energy reduction. Because of the influence of design on energy consumption, the optimal design should be employed to take advantage of energy savings opportunities.

To effectively apply LW to MTs, it is important to have an understanding of where energy is consumed. The focus of this paper will be on vertical milling MTs due to the significant number of vertical mills currently being used and the projected market growth being $8.77 billion in 2026 from $6.91 billion in 2018 [12] (see Fig. 1(*a*) for a schematic of a vertical mill). Figure 1(*b*) shows a "standard" power profile for a vertical milling machine; the area under the power curve is the energy consumed. As is evident, the profile can be decomposed into four components. When the MT is turned on, the power consumption spikes and then quickly falls to a steady-state; this steady-state is the first component: basic power. Basic power is associated with devices and systems that are switched on when the machine is powered, e.g., computer, fans, lubricant system, and the control system. Then, the spindle and table feed drives are engaged, and the feed drives move the table in the *x*- and *y*-directions (Fig. 2). Another spike in the power occurs associated with the spindle start-up (often the spindle is started before the table drives are engaged). The power quickly drops down to another steady-state which is the second component, the spindle rotation, and feed power. A third component of the power profile occurs when the cutting tool engages with the workpiece: cutting power. This power is associated with moving the table while the workpiece material is being cut. When

[1]Corresponding author.

Manuscript received September 24, 2020; final manuscript received March 2, 2021; published online April 26, 2021. Assoc. Editor: Karl R. Haapala.

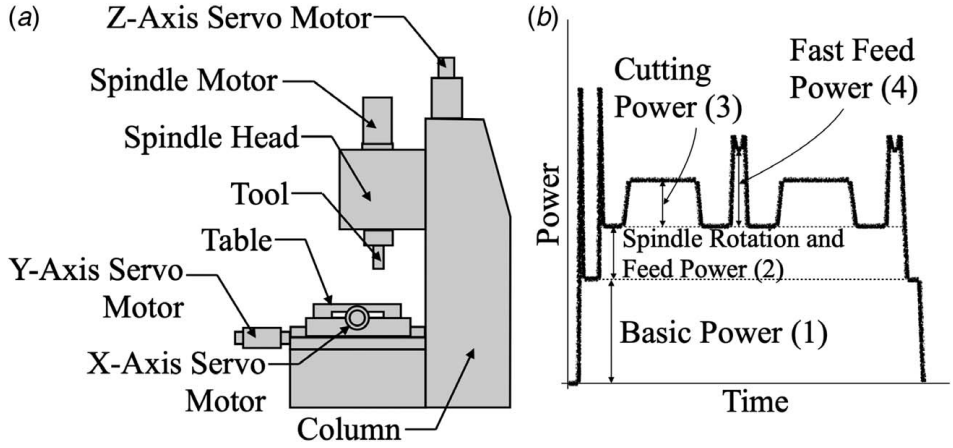

Fig. 1 (*a*) Schematic of a vertical milling MT, adapted from Triebe et al. [13], and (*b*) power profile of a milling machine, adapted from He et al. [14]

cutting ends, the cutting power component is eliminated. A fourth power profile component often occurs, fast feed power. This is associated with the table moving quickly during the rapid traverse. After cutting is completed and the table is moved back to the starting position, the spindle rotation and feed power are eliminated. Then, when the machine is turned off, the basic power component is also removed. From this figure, it can be seen how the speed of the table can greatly influence the MT's energy consumption, see power component 4, fast feed power. With the desire for faster throughput, faster feeds will be used and therefore greater energy consumption and greater potential for LW to reduce energy consumption.

To seize upon the benefits offered by the optimal design and LW, the objective of this paper is to establish a method that may be used to minimize the energy consumption of an MT through mass reduction. This is accomplished by replacing a solid MT slide table with a sandwich structure (the proposed method will optimize the structure). A representative slide table is shown in Fig. 2. The table was chosen for LW for the reasons stated earlier. In many vertical milling MTs, the table moves throughout the use of the MT which contributes to power components 2, 3, and 4 in Fig. 1(*b*); to cut in the *x*- and *y*-directions the slide table moves. Therefore, a reduction in the mass of the slide table will reduce the power of these three components and the energy attributed to them. However, mass reduction often leads to a loss of stiffness. Therefore, both mass and stiffness must be considered. To design the lightweight table, the proposed method optimizes the shape of the sandwich structure core to minimize mass and maximize stiffness. To accomplish this multi-objective optimization, a Non-Dominated Sorting Genetic Algorithm (NSGA-II) proposed by Deb et al. [15] is used to find the optimal core shape. NSGA-II was chosen for its ability to accommodate multiple objectives, preserve the diversity of the population (wide range of solutions), and search various regions of the solution space simultaneously.

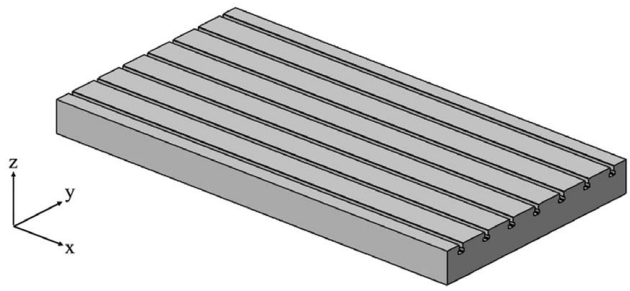

Fig. 2 Slide table

Given this brief introduction, the remainder of the paper is structured as follows. First, an overview of LW will be given. Then, the optimization method will be described including assumptions made, how the core is generated using a genetic algorithm (GA), and the different objectives considered. Next, the results from the GA will be shown and discussed. Finally, the paper will summarize and state conclusions.

2 Literature Review

This paper explores the use of LW to reduce the energy consumption of an MT. With this in mind, this section briefly reviews past efforts related to LW in several product design contexts. In particular, this section will review LW methods in the transportation sector and with respect to MTs.

2.1 Overview of Lightweighting in the Transportation Sector. LW has had success in the transportation sector due to the direct connection between mass and fuel consumption. Due to the clear successes of LW in automobiles and aircraft, literature where LW has been applied to automobiles and aircraft is reviewed, with an eye toward MT applications. Most LW design strategies for automobiles and aircraft adopt one of three approaches, where it is to be noted that there is some overlap among these approaches: lighter materials, LW via manufacturing, and LW via product structure. While it is evident that the third approach is design-oriented, the other approaches often require design changes as well, e.g., dimensional changes due to differences in material properties. Material LW seeks to replace a current material with a lighter-weight (lower density) material. Manufacturing LW encompasses manufacturing methods that help reduce mass through lighter parts or assemblies. LW through structural changes involves creating a design that reduces mass through a stronger but lighter structure or a reduced number of components.

2.1.1 Materials. There are a number of materials-focused design strategies that may be pursued with respect to LW. These include the use of high-strength steel (HSS) [9,16,17,18], aluminum alloys [17,19], magnesium [17,20], and polymers and composites [9,17,21]. The use of these alternative materials allows for either less of similar material to be used, i.e., HSS, or a lighter material that provides similar strength. For example, although HSS is not a lightweight material, it still can achieve weight savings of 15–26% [17]. In the case of automobiles and aircraft, materials-focused strategies can be accomplished through a number of areas. For example, in automobiles, thinner walls can be achieved in the outer skin, floor panels, frame, chassis beams, and seat rails [16]. Aluminum can be used in areas of the automobile such as the

roof, door, floor, and structural components like knuckles [17]; often, cast aluminum alloys are replacing ferrous alternatives. For aircraft, aluminum alloys are widely used [17]. For example, aluminum-lithium alloys are being used in airframes of aircraft [17]. In automobiles, magnesium has potential in applications such as engine block, steering column, steering wheel, door inners, seat frame, and instrument panels [17,20]. In aircraft, magnesium alloys are used in castings to reduce weight. Titanium alloys are used in aircraft structures, fasteners, structural forgings, and fittings. Composites are another lightweight engineering material commonly used in automobiles and aircraft (e.g., Boeing 787) [9,17,21]. In automobiles, composites have been used in supporting roof pillars, door frames, chassis, body panels, fenders, and wheelhouses [17]. In aircraft, the focus has been on replacing secondary structures, structures that are not load-bearing and not directly critical to flight, with composites [21]. This includes panels for the fuselage, clips, brackets, seatbacks, window panels, and cockpit floor. It should be noted that the use of alternative/lighter materials is not a "one-to-one" replacement. Other design changes, such as dimensional changes, must be implemented due to the difference in the properties of the original and replacement materials.

2.1.2 Manufacturing. Manufacturing provides multiple design strategies for LW automobiles and aircraft [17,18,22]. These include the use of tailor-rolled blanks, hydroforming, hot forming, vacuum-assisted die castings, semisolid thixo-forming, extrusions, high pressure die casting, and additive manufacturing (AM). Tailor-rolled blanks allow for variation in sheet thickness to reinforce where needed and reduce weight where the thickness is not needed. Hydroforming uses hydraulic fluid to press metal into the desired shape. This method allows for complex, structurally strong shapes and helps reduce the number of parts. Hot forming allows for the forming of high-strength materials in which their formability increases significantly at high temperatures. Vacuum-assisted die castings allow for the integration of several parts with good dimensional accuracy, surface finish, and mechanical properties. Thixo-forming is a semisolid processing method that can produce complex shapes at low temperatures. The extrusion process enables the mass production of complex designs. High pressure die casting is a cost-effective process that allows for the production of high-volume metal parts with tight tolerances. AM allows for novel geometries that could not be accomplished with traditional manufacturing methods. Other manufacturing methods more common in aircraft production include integral milling of pockets, cutouts and lightening holes, and local thinning by chemical milling [17]. Similar to material changes, the use of different manufacturing methods usually requires other design changes due to the differing capabilities of the methods and the differences in the geometries of the new parts.

2.1.3 Product Structure. LW via product structure in automobiles and aircraft can be accomplished through a number of methods which include topology analysis [9,18], system optimization [17], shell design instead of frame construction [9], and fewer subassemblies and fasteners [17]. Topology optimization can provide an initial structure to analyze and an initial design to start from. System optimization reduces the number of parts and fasteners in an assembly or system. This can be accomplished through the use of various manufacturing methods including AM, bonded structures, co-cure co-bonded composites, and single molded large structures. Shell designs replace frame constructions to reduce mass and are accomplished through the use of manufacturing techniques as stamping and welding [9].

An example that incorporates these three LW design techniques for the LW of automobiles is the 2015 Ford F-150. This vehicle used more lightweight materials with design changes to reduce the mass by 300 kg [17]. An example for LW aircraft is the design of the Boeing 787 in which the primary structure is made up of as much as 50% composite while a previous model 777 was made up of only 12% composite by weight [23]. Because of this use of composites to reduce mass, the aircraft is up to 20% more fuel-efficient.

2.2 Lightweighting in Machine Tools. LW of MTs has the potential to reduce their energy consumption along with other benefits. Kroll et al. [8] summarized the benefits of LW as being a decrease in reactive energy (related to inertial forces) and friction losses, and an increase in acceleration capability, process stability, and responsiveness. The authors modeled motor energy loss based on acceleration and mass and showed a reduction in mass leads to a reduction in motor energy loss. The authors also summarized the LW potential for various types of MTs with laser cutting equipment having the greatest potential and a grinding machine having the least. Herrmann et al. [9] reviewed the lifecycle impacts of lightweight structures including the potential impact reduction during the use stage. The authors stated that the increase in energy efficiency, when applied to moving masses, can offset potential increased impacts during material extraction and manufacturing.

To accomplish LW in MTs, there have been a number of design strategies. One of these strategies includes the use of composites. Möhring [24] gave an overview of the design and application of composite materials in MTs. One application covered was the use of composites in spindles and tools to reduce the inertia (I) of the spindle rotors and tool bodies, and reduce their thermal growth and improve their dynamic behavior. The author also examined the application of composites for slide structure and clamping systems. Neugebauer et al. [25] looked at a hybrid carbon fiber reinforced polymer (CFRP) ball screw drive; the ball screw drive had lower inertia (I) that translates into lower electrical losses and higher drive dynamics. It also has about 10 times lower thermal expansion than a conventional metallic ball screw. Suh et al. [26] constructed composite slides for a large computer numerical control (CNC) MT by bonding high-modulus CFRP composite sandwiches to welded steel structures. These composites reduced the mass of the horizontal and vertical slides by 26% and 34%, respectively, and increased damping by 1.5–5.7 times without sacrificing stiffness. Sulitka et al. [27] applied composites and sandwich structures to the crossbeam and columns of a gantry MT. The total x-axis moving mass was reduced by 35%, and the total crossbeam and column mass was reduced by 52.3%. Because of this reduced mass, the authors were able to employ a smaller motor that used 20% less power. Merlo et al. [28] substituted electro-welded steel structures in the column and ram with a hybrid sandwich structure made of steel facing plates with a core of CFRP and aluminum honeycomb. Damping was increased by up to three times for the ram and eight times for the column while mass was reduced by 20% for both. For a second case study, the authors substituted the steel ram with one made of a hybrid material structure. The skin was thin steel plates that were glued on an internal tube fabricated through filament winding technology. Mass was reduced by 40% and damping increased by 2.5 times.

In addition to the use of CFRP, mass can be reduced through the use of other lightweight materials. Lv et al. [29] explored reducing the inertia (I) of the spindle by reducing the mass of the chuck through an aluminum design that reduced the mass by up to 60%. The authors chose to focus their efforts on the chuck instead of the spindle in order to retain stiffness in the spindle. The authors found the inertia (I) of the spindle system dropped from 0.3354 to 0.2380 kg-m^2 which reduced peak power and energy consumption by 21.2% and 20.6%, respectively. Dietmair et al. [30] redesigned a milling machine by employing steel and aluminum foam sandwiches to reduce the mass of the ram. The mass was reduced by 15%, and the structural damping coefficient was increased by 250% while the static stiffnesses in the x and z-directions were sacrificed by 10%. The authors also investigated reducing the weight of the milling head by replacing the steel with aluminum which reduced its weight by 27%. Other design changes the authors explored included reducing the inertia of the drive chain, lower power motors and converters, and advanced instrumentation and

control. With all these changes, the authors were able to reduce the moving mass in the y- and z-axes by 16% and 18%, respectively, and reduce the motor power in both axes by 40%.

Other LW methods include structural design changes. Zulaika et al. [31] explored reducing the mass of the ram through thinner wall thickness while increasing stiffness via additional/redundant guideways in the vertical guiding system of the frame. The authors redesigned the ram based on modeling the interactions between the representative milling operation and the machine dynamics. Li et al. [32] designed a new grinding machine column with a focus on enhanced stiffness and decreased weight using a branching pattern of leaf venation as inspiration. The maximum deformation was reduced by 23.60% and weight reduced by 1.31%. Zhao et al. [33] designed a tool column with improved static and dynamic performance using a structural bionic method. This design was based on configuration principles from bone and plant stems and was able to decrease mass and deflection by 6.13% and 45.9%, respectively. Zhao et al. [34] designed a lighter working table of an MT using three construction types: hollow stem, sandwich node, and radial root. The fuzzy assessment was used to decide when which method should be used. Triebe et al. [35] also developed a method to reduce the mass of the working table in an MT through GA. The solid table design was changed to a sandwich structure and the method optimized parameters of the sandwich design, such as the thickness of the cell wall and height of the core. A Pareto front (PF) was made for two different designs, honeycomb core and foam core, and compared to a solid plate. Li et al. [36] designed a lighter-weight and stiffer MT bed through the topology. The authors developed a simplified spring model composed of shell and matrix elements to simulate a real bed structure. The finite element method was employed to identify the load-bearing topology. The final design reduced the maximum deformation by 19%, and the transverse stiffness was improved by 7.82%.

Having provided background on LW strategies employed with automobiles, aircraft, and MTs, this paper will now shift to the proposed method of LW and design optimization. The following section will describe the application of GA to reduce the mass of an MT.

3 Application of Genetic Algorithm to Table Design

With an understanding of past efforts relating to MT energy consumption and LW design strategies for reducing mass and thus energy, attention now shifts to applying the LW concept to an MT table. An example of a sliding table can be found in Fig. 2. Drawing on successes from LW in transportation and previous MT research, a sandwich structure design will be explored to replace the solid table construction shown in Fig. 2. A sandwich structure has been chosen due to its lightweight yet strong characteristics. The sandwich structure will draw from manufacturing advances covered in Sec. 2 by using a single row of cells for the core structure that have the potential of being economically manufactured, see Fig. 3 for an example. Figure 3 shows a sandwich structure consisting of square cells along with other potential cell shapes. These various cell shapes will change the properties of the table and therefore should be investigated.

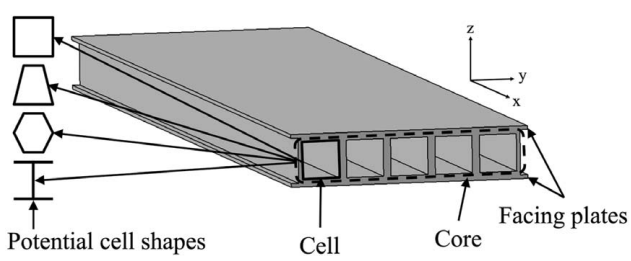

Fig. 3 An example of a sandwich structure configuration

To design the sandwich structure, a biologically inspired optimization method, GA, will be utilized. This specific algorithm to be employed is NSGA-II. GA will allow for the optimization of the core with respect to multiple objectives (more description of the method can be found in the study by Deb et al. [15]). GA allows for the finding of multiple optimal solutions, as opposed to a single solution, and reduces the chance of getting stuck at a local optimum. This particular algorithm, NSGA-II, better maintains a diversity of solutions instead of congregating at one end of the optimal spectrum. The main goal for this GA is to reduce the mass of the table; however, with reducing mass, there is the potential of reduced strength. Therefore, strength will be a secondary consideration in the optimization procedure. The core is optimized through the shape of the cells that affect the mass and strength of the table. NSGA-II will choose optimal shapes for the cells to reduce mass but maintain the strength of the sandwich structure. The profile of the cells along with the wall thickness will be chosen.

An illustrative example will be considered to demonstrate an application of the GA method. This will be accomplished through a model of the table slide for a vertical milling machine, e.g., Hurco VMX64i. The table dimensions are $889 \times 1676 \times 89$ mm (width × length × height) with the core height being 76 mm and both of the facing plates having a thickness of 6.4 mm. The material of the table is steel, ASTM-A36. For simplification, T-slots were not included in the analysis.

3.1 Generation of Cell Shapes. Since the shape of the cells is being optimized, the chromosomes were defined as the cell shape. The chromosomes are made up of y and z coordinates of each individual point of the cell profile (20 points total) and the thickness of the profile. An example cell profile can be found in Fig. 4(*d*) with an explanation of chromosome generation to follow. To form the shape, the points are arranged in a counterclockwise fashion with each point being connected to the next in the chromosome; i.e., the first is connected to the second which is connected to the third and so on. The final y–z coordinate is connected to the first, which produces a closed shape. The final value in the chromosome is the thickness of the profile which ranges from a solid cell to a wall thickness of 2.5 mm. To generate each shape, the following procedure is used, see Fig. 4 for more detail (Fig. 4 shows a total of 14 points ($n = 14$) instead of 20 for ease of viewing):

(1) First, four fixed points are generated creating a rectangle. The generated rectangle has a width of 13 mm and a height of 76 mm, matching the core height. This creates flat areas to which the upper and lower plates can be attached. These four points are always 1, $n/2$, $n/2 + 1$, and n (see Fig. 4(*a*)) and will never move throughout the generations.
(2) The next points generated are immediately to the right of points 1 and $n/2$ (2 and $n/2 - 1$) and to the left of $n/2 + 1$ and n ($n/2 + 2$ and $n - 1$, see Fig. 4(*b*)). These points determine the width of the top and bottom of the cells. These y-value coordinates of these points can be in the range of 6.5 mm from the center (location of the first four points) to 51.5 mm from the center (the maximum width of the shape). The z-value coordinates are 0 mm for the bottom two points and 76 mm for the top two points. During recombination and mutation, these points can move horizontally, but not vertically, between these two boundaries.
(3) The rest of the points are generated randomly horizontally between the maximum width and the minimum thickness; however, their vertical, z-direction, positions are predetermined, see Fig. 4(*c*). The vertical position of each point is based on where the point lies in the chromosome. Throughout the generations, these points can move horizontally between these boundaries.

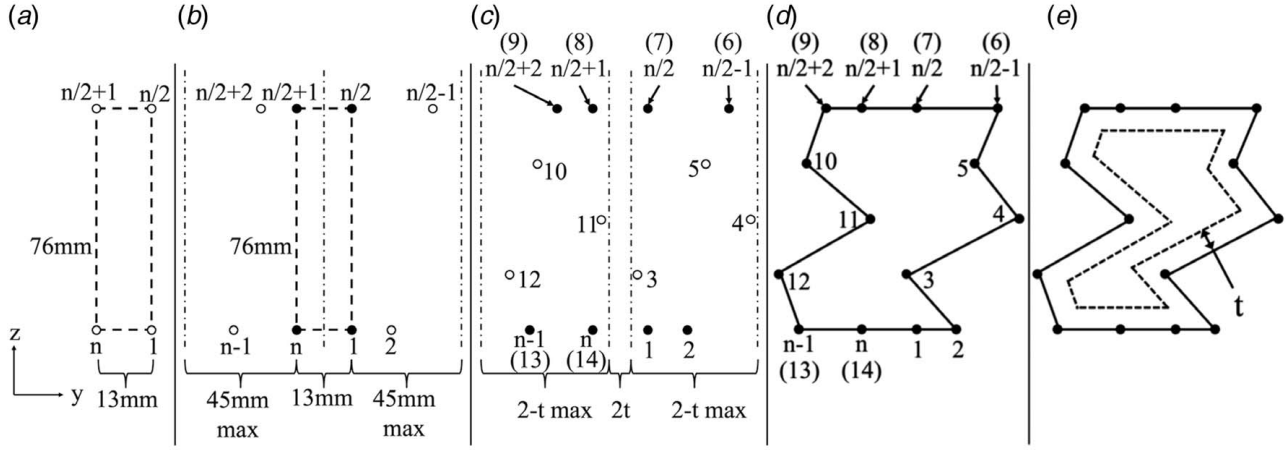

Fig. 4 Shape generation procedure (14 points shown instead of 20 for ease of viewing) described in steps 1–5 of Sec. 3.1

(4) Once all points are generated, they are connected from 1 to 2, 2 to 3, and so on till n with point n being connected to 1 to create a closed shape. This can be seen in Fig. 4(*d*).
(5) Finally, the inner profile is made using the outer profile and the thickness value, labeled as t in Fig. 4(*e*), within the chromosome. The thickness is initially a random value between 2.5 and 50 mm, which creates a solid cell, for each shape. During recombination, the thickness is averaged between the two parents, and during mutation, the thickness is modified by a random number between the +/− mutation distance divided by 2.

3.2 Objective Functions. The first of the objective functions is the mass of the sandwich structure table. To calculate the mass, the area of a single cell is found through the profile and thickness and then multiplied by its length and by the density of the material, ASTM-A36. The mass of a single cell is then multiplied by the number of cells required to fill the core horizontally. This can change depending on the width of the cells. Finally, the mass of the outer plates is included.

Two objective functions were created to consider the strength of the table: an expression for the moment of inertia I, and an equation for the polar moment of inertia J. These objective functions relate directly to bending, along the x-axis, and torsion, around the x-axis, of the table, which are two indicators used for measuring the strength of the sandwich structure in this paper; the larger I and J are, the less bending and torsion in the table, respectively. From looking at a free body diagram of the table, shown in Fig. 5, it is seen how the forces applied by the drive system (e.g., lead screws) along with the cutting forces and force due to gravity can produce bending and torsion in the table. I and J of the table were calculated about its centroid. The centroid can be found through integrating across the area (A) using Eq. (1). Once the centroid is found, I and J may be calculated. I, in this case, is equal to the moment about the y-axis, is calculated by Eq. (2), while J, found by Eq. (3), is equal to the moment about the y-axis (Eq. (2)) plus the moment about the z-axis (Eq. (4))

$$\bar{y} = \frac{\int_A y \cdot dA}{\int_A dA}, \bar{z} = \frac{\int_A z \cdot dA}{\int_A dA} \tag{1}$$

$$I_{\bar{y}} = \int_A z^2 \cdot dA \tag{2}$$

$$J = I_{\bar{y}} + I_{\bar{z}} \tag{3}$$

$$I_{\bar{z}} = \int_A y^2 \cdot dA \tag{4}$$

The fitness objectives for the GA include the mass and the values for I and J. I and J were modified because I_z was naturally much larger than I_y due to the table being a long rectangle. Therefore, I was modified by multiplying I_y by 100 to provide similar scaling in the optimization procedure to I_z, see Eq. (5). J was also modified by multiplying I_y by 100 to provide similar scaling (Eq. (6)). These two modifications ensure that the different objectives have comparable values in the GA fitness function. To summarize, the objective functions include the mass of the table, I_{mod} (Eq. (5)) and J_{mod} (Eq. (6))

$$I_{mod} = 100 I_{\bar{y}} \tag{5}$$

$$J_{mod} = 100 I_{\bar{y}} + I_{\bar{z}} \tag{6}$$

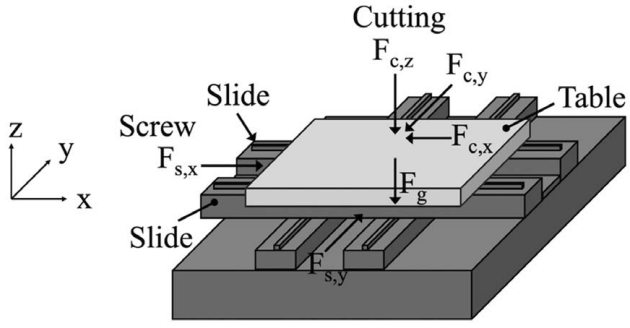

Fig. 5 Free body diagram of the slide table

4 Results From Genetic Algorithm

The GA was run for 100 generations (not much improvement was seen after that), and the values for mass, I, and J were recorded for all the solutions in the final population. I_{mod} and J_{mod} were not recorded since they were needed only during the optimization process and do not represent the true moment of inertia and polar moment of inertia. These members of the population establish the PF shown in Fig. 6. This figure shows how the population approached an optimal front. To further show the convergence of the population, the GA was run for 500 generations to build an equation representing the optimal PF. Then to represent a fitness value for each generation, the average distance of the whole population to the PF representation was found. This was accomplished

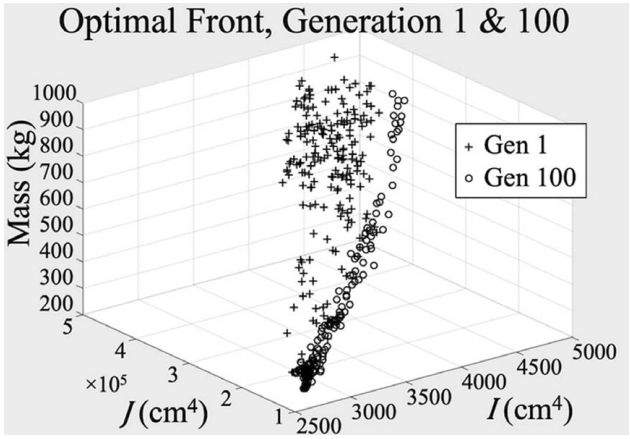

Fig. 6 Optimal PF compared to first generation

by finding the distance of each point to the representative PF and taking the average for each generation. This average distance was plotted for all 500 generations (Fig. 7). Using this method to visualize the fitness, it can be seen that at generation 100 the population converged to the representative PF front with little improvement seen in later generations. In all cases, the cell shapes converged to a cross section that resembles an I-beam, a set of I-beams that form the table. This is not unexpected since I-beams handle bending very well. The points with the large mass in Fig. 6 tend to be bulkier but have better stiffness than the ones with the smaller mass. Examples of how these shapes will work in an MT table are shown in Fig. 8.

Since the shapes generated from the GA may be difficult to manufacture at a low cost, the authors compared standard shapes to what the GA generated. For example, a table constructed of square tubes and one built from I-beams were considered. It was found that these two designs had slightly smaller J values, but comparable mass and I values, as shown in Fig. 9. These standard shapes include rounded corners that avoid stress risers associated with sharp corners. The practical indications of this are that common extrusion and tube shapes, I-beam or square beam, can be used to build the table.

To model the strength of the sandwich structure design, several finite element analyses (FEA) were performed. Three table designs were analyzed (see Fig. 10). The first design, Fig. 10(*a*), had a core constructed of I-beams, same as standard I-beam shown in Fig. 9, running in the x-direction of the table, the second design, Fig. 10(*b*), had a core of I-beams running in the

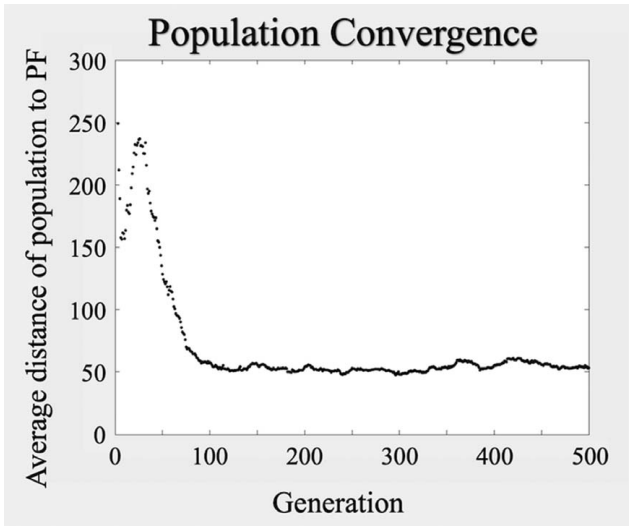

Fig. 7 Average distance of population to the representative PF

y-direction, and the third design, Fig. 10(*c*), had a solid core. All three table designs were modeled with T-slots.

To model the loading conditions, first restraints were placed where the guides would be. Then, a force due to table mass was distributed across the whole table, and a force associated with the mass of the workpiece (a distributed load of 26,700 N) was applied evenly over the top face of the table. Then, a cutting force of 1800 N in the x-direction, 1800 N in the y-direction, and 900 N in the z-direction was applied. The nine locations to which this set of cutting forces were applied are shown in Fig. 11, and the FEA was run for each of these nine applied force locations. The magnitude of the deflections measured in micrometers of these various FEAs can be found in Table 1. The I-beam table designs have greater deflections than the solid design, however, still very small. These FEAs must be considered in the design of the table, and if the table design does not meet certain requirements, then stiffeners may need to be added or a thicker core used. It is worth noting that these simulations were run at a worst-case scenario due to the max designed load on the table. Therefore, under normal cutting conditions, the tables would have even smaller deflections.

To further explore the design of the table, a sensitivity analysis was performed on the x-axis I-beam table design. The four feature dimensions for the I-beam shown in Fig. 9 were increased and decreased by 10%. An FEA was performed for each of these scenarios at loading position 1, from Fig. 11. Loading position 1 was chosen since most cutting will take place near that location. These results can be found in Table 2. A positive result indicates an increase of deflection or mass, and a negative result indicates a decrease in deflection or mass. This analysis shows decreasing height and increasing width of the I-beam both decrease deflection and mass. There are other options to decrease the deflection, but these end up increasing the mass. It should be noted that both the increasing and decreasing width of the I-beam decreased the deflection. The increasing of the width increases the area of the I-beam that bears the load and therefore produces a stronger I-beam, up to a certain point. The decreasing of the width allows for more I-beams to fit across the core of the table which would understandably increase the stiffness of the table and also the mass.

From these two designs, the x-axis and y-axis designs found in Figs. 10(*b*) and 10(*c*), about 50% mass savings is accomplished in the table. This is significant since the table will constantly move throughout the cutting of the workpiece. This method of LW meets and exceeds other LW applications reviewed in Sec. 2.2 when comparing mass savings. Other methods had a mass savings from as low as 15% [30] and up to 60% [29]. However, due to their different applications, energy savings will vary significantly. For example, the application of mass savings in the chuck [29] has great potential for energy savings due to the constant movement and high acceleration and deceleration of the spindle. In addition, this method of LW the table has the potential to be of lower cost due to the use of more common materials and manufacturing processes, e.g., rolling of steel I-beams. Other methods require more complex and expensive materials such as CFRP. However, to better compare energy savings due to LW, the link between mass and energy in the table should be further explored. The next section will discuss the energy reduction potential along with design considerations.

5 Discussion

A reduced mass of moving components reduces energy consumption. However, when changing the mass of the MT, additional design changes are necessary, similar to what was shown in Sec. 2.1. These additional design changes include revisiting components that move and support the table, e.g., slides and ball screws. This section will first discuss the energy reduction potential followed by the necessary design changes, specifically, the motors driving the table.

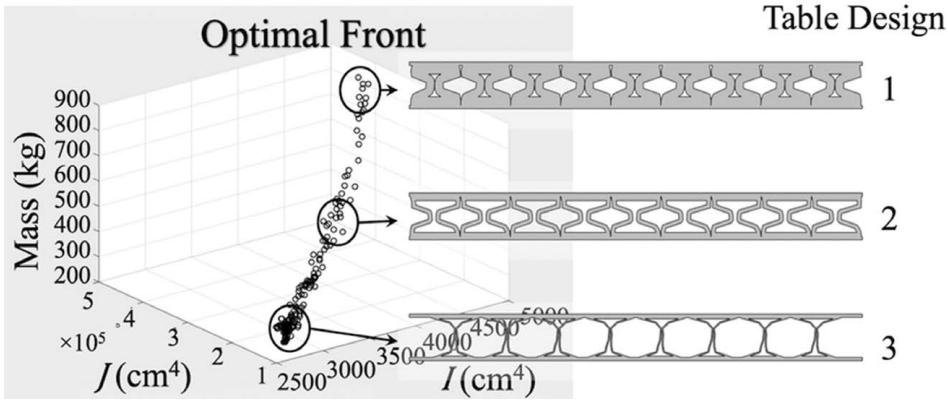

Fig. 8 Table design examples

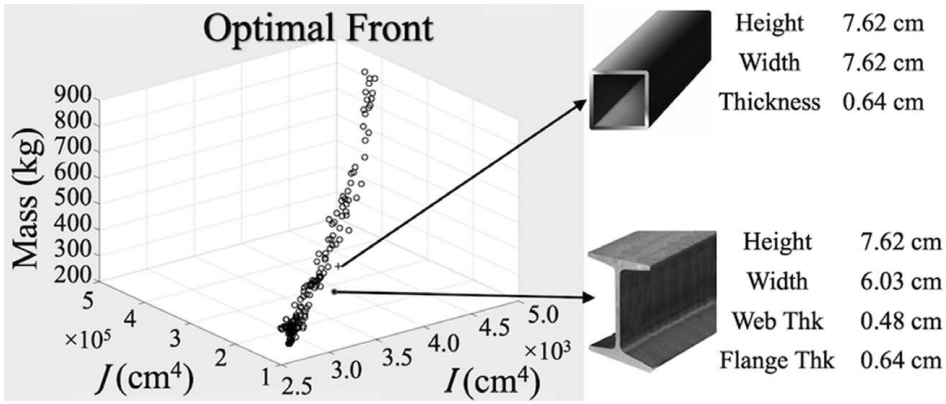

Fig. 9 Standard shapes comparison

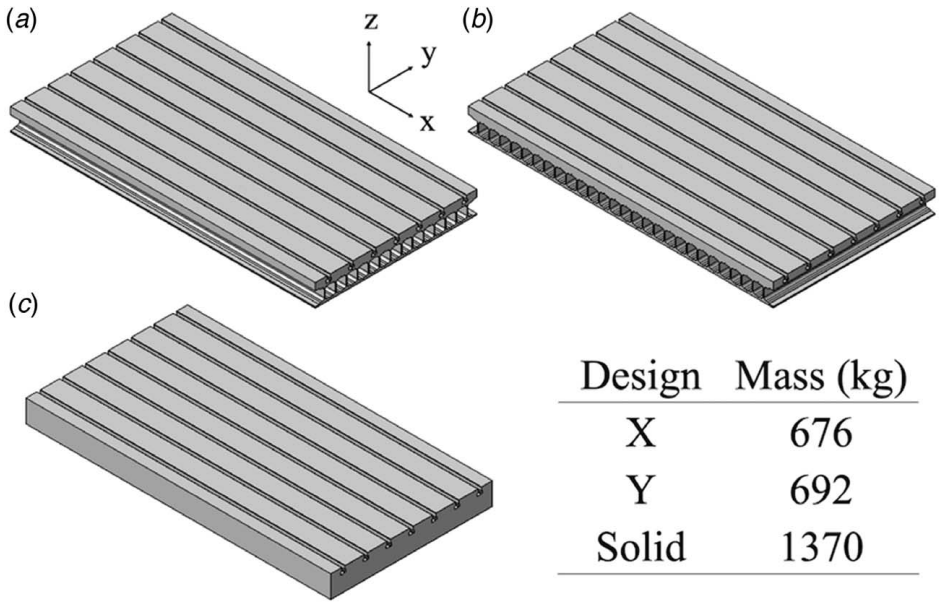

Fig. 10 Table designs used in FEA: (*a*) *x*-axis running beams, (*b*) *y*-axis running beams, and (*c*) solid table

5.1 Energy Reduction. In moving a MT table, three stages must be considered: table acceleration, constant velocity, and table deceleration. In all three stages, mass plays a role in the driving force required and thus the energy consumed. Decreasing the mass will decrease the force and therefore the required energy to move the table. The mechanical energy equation and its components can be seen in Table 3. η_s is the ball screw efficiency while μ is the coefficient of friction for the ways.

For electrical energy, it can also be seen as to why mass would play a role in reducing energy consumption for a motor. This can

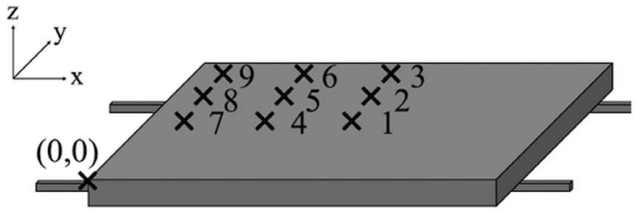

Position	X	Y
1	838.2	469.6
2	838.2	670.56
3	838.2	863.6
4	425.45	469.6
5	425.45	670.56
6	425.45	863.6
7	25.4	469.6
8	25.4	670.56
9	25.4	836.6

Fig. 11 Loading positions, due to cutting, for the various FEA simulations. Position coordinates in millimeter.

Table 1 Magnitude of deflection in μm at each loading position from the FEA simulations

Table design	Position 1	Position 2	Position 3
X	1.136	1.298	4.465
Y	0.977	1.104	2.483
Solid	0.569	0.701	0.894
	Position 4	Position 5	Position 6
X	1.200	1.296	4.660
Y	0.843	1.014	2.591
Solid	0.480	0.780	0.856
	Position 7	Position 8	Position 9
X	1.587	1.948	8.554
Y	1.212	1.842	5.319
Solid	0.706	0.840	1.360

Table 2 Sensitivity analyses conducted on the *x*-axis I-beam table design

		Change in	
Feature		Deflection	Mass
Height	+10%	+0.185	+6.694
	−10%	−0.035	−6.695
Width	+10%	−0.032	−1.897
	−10%	−0.032	+13.889
Web	+10%	−0.035	+13.889
	−10%	+0.050	−5.574
Flange	+10%	−0.043	+10.851
	−10%	+0.078	−10.708

Note: Each feature of the I-beam was modified by +/−10% with the change in deflection (μm) and mass (kg) recorded. The analysis was run at position 1 (see Fig. 11).

Table 3 Mechanical and electrical energy equations

	Mechanical energy ($E = Fx/\eta_s$)	Electrical energy ($E = P_{in} \cdot t$)
$F = F_{acc} + F_v + F_{dec}$	$x = x_{acc} + x_v + x_{dec}$	$P_{in} = V_{out} I$
$F_{acc} = ma_{acc} + \mu mg$	$x_{acc} = \frac{1}{2} a_{acc} t_a^2$	$P_{out} = T \cdot n$
$F_v = \mu mg$	$x_v = vt_v$	$\eta_m = P_{out}/P_{in}$
$F_{dec} = \mu mg - ma_{dec}$	$x_{dec} = \frac{1}{2} a_{dec} t_d^2$	$I = \frac{T}{K_T}$
		$T = \frac{Fl}{2\pi\eta_s}$

be seen in Table 3. These equations are for a direct current (DC) motor, but the role of mass with respect to energy is similar for an alternate current (AC) motor. For a DC motor, much of the time the output voltage, V_{out}, is constant. It is set by the manufacturers of the motor. The current will change based on the required torque. K_T is the torque constant, l is the ball screw lead, and η_s, as stated before, is the ball screw efficiency. P_{out} is the output power, and η_m is the motor efficiency which depends on the ratio of the input power to the output power. This motor efficiency is based on the design load of the motor.

Choosing the right motor for the application is very important. This is because if motors are run below their designed load, or rated power, they will run less efficiently. Motors normally operate more efficiently at 75% of their rated load and above [37]. Motors that run at 50% or less of their rated load operate inefficiently due to the reactive current increase and power factor decrease. An example of this behavior can be seen in Fig. 12. Saidur [37] found that many motors are not properly sized; in fact, Capehart et al. [38] found that 75% of all motors have a load factor of less than 60%. With the reduction of mass in the table, there is a reduction in the required load for the motors to drive the table, which will lower the load factor. With this in mind, there is potential that a design change must be made in regard to the motor size.

To size the motor, a number of characteristics are needed. First the load, or required torque, should be known. Every motor has a continuous torque rating that the motor can run at indefinitely and a peak torque rating that the motor can run at for a short amount of time before overheating. Other specifications that should be known before choosing a motor include inertia/mass of the load, required speed, and required acceleration. Here, we will focus on torque and inertia/mass. Standard running speeds of machine tool

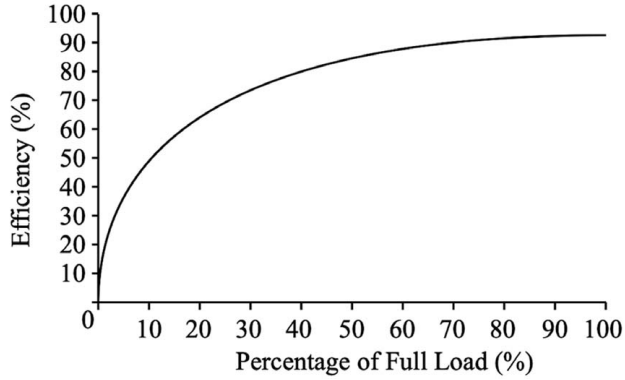

Fig. 12 An example of a relationship between motor loading and efficiency [37]

tables can be calculated based on recommended cutting conditions from cutting tool manufacturers. Standard accelerations can be found from motor manufactures.

For inertia and mass, more than the mass of the table should be considered, this includes the mass of the workpiece and the inertia of the ball screw. To calculate torque, the required force, lead of ball screw, and screw efficiency should be known (see Eq. (7)). The force equations can be found in Table 3. Using a standard running condition along with extreme running conditions, the continuous torque and peak torque, and continuous power and peak power can be found. Then, using those values, along with the required speeds of the motor, a motor can be chosen using torque–speed curves. There are other considerations to be made, such as inertia ratio, but the current focus of this paper will be torque, speed, and power

$$T = \frac{Fl}{2\pi\eta_s} \tag{7}$$

Using the equations in Table 3 along with some assumptions as to an "average" velocity profile, energy savings may be calculated. Using a trapezoidal speed profile as a representative behavior together with rapid traverse during a portion of the movements, along with values for feed, speed, acceleration, and other values from MTs taken from CAM software and MT builders, energy savings were calculated. For a mass savings of 500 kg, about 1 kWh is saved per day. This means about 2 Wh is saved per 1 kg of mass reduction. However, for this energy savings to be realized, the motor must be properly sized. From the method outlined in this section, looking at required loads and speeds, a continuous torque and peak torque along with continuous power and peak power were found for the new, lighter-weight, table configuration. The power rating of the motor must be reduced by 10% to achieve these energy savings; otherwise, the motor will be oversized and may run inefficiently. Due to the varying types of MTs and parts to cut, e.g., size, material, features, a more detailed analysis would be needed to quantify the energy savings for a particular MT.

6 Summary and Conclusions

This paper proposed a method to assist in the design of lightweight MTs. LW MTs have the potential to reduce the environmental impact of manufacturing by reducing the energy consumed by an MT. This reduction comes from reducing the power required to move a mass and properly sizing the motor for the application. To accomplish this LW, the authors proposed replacing the solid table of an MT with a sandwich structure. The core of the structure would be made up of cells running horizontally along the x-axis of the table. The manufacturing of the sandwich structure table would be relatively straightforward.

Optimization of this table was accomplished through a GA. Specifically, the core of the sandwich structure was formed through the use of joined beams, where the cross-sectional shape of each beam (cell shape) was optimized through multi-objective optimization via NSGA-II where mass and strength were the objectives. The strength objectives were represented by I and J of the table since they relate directly to bending and torsion, respectively. The fitness of any solution is based on the three objectives: mass, I, and J. The program was run through 100 generations, and a PF was generated from the results of the objective functions for each table design. The optimized shapes ended up being similar to I-beams; this is not surprising since I-beams are very resistant to bending.

The optimized table designs provided mass savings that ranged from 216 to 777 kg. Two table designs were modeled using FEA and were shown to have similar stiffnesses to a solid table design. The lighter-weight table would save energy since smaller forces would be required to move the table. To achieve the energy savings from LW, the motors that drive the table must be resized too.

This paper has made a number of key contributions related to lightweight MTs for energy savings as follows:

- For the first time, an LW MT application is considered for energy savings that is accomplished through the replacing of the solid table with a sandwich structure.
- A multi-objective problem is solved through a genetic algorithm that optimizes the core of a sandwich structure table with the objectives of minimizing mass and maximizing I and J.
- A novel shape generation method is proposed to find the cross-sectional members of a set of parallel cross sections in a sandwich structure. This method allows for the generation of many different shapes and ease of integration into GA.

Future research directions will include the use of this method in actual design with the selection of motors taking into account the inertia and speed/torque requirements of the drive system. A more detailed relationship between mass and energy will then be explored. Dynamics and vibration will be investigated as well due to the potential concerns of the changing natural frequency of the table. Finally, this method will be applied to other moving components within the MT including the spindle.

Acknowledgment

This work is supported in part by the U.S. National Science Foundation (Grant No. 1512217). Any opinions, findings, conclusions, and/or recommendations expressed are those of the authors and do not necessarily reflect the views of the U.S. National Science Foundation.

Conflict of Interest

There are no conflicts of interest.

Data Availability Statement

The data sets generated and supporting the findings of this article are obtainable from the corresponding author upon reasonable request. The authors attest that all data for this study are included in the paper.

References

[1] Central Intelligence Agency, 2017, "The World Factbook: Economy—Overview." Washington, DC, https://www.cia.gov/library/publications/resources/the-world-factbook/geos/print_xx.html
[2] LLNL, 2020, "Energy, Water, and Carbon Informatics," https://flowcharts.llnl.gov/
[3] IEA, 2019, "Total Primary Energy Supply by Fuel, 1971 and 2017," Paris. https://www.iea.org/data-and-statistics/charts/total-primary-energy-supply-by-fuel-1971-and-2017
[4] US EIA, 2019, "December 2019 Monthly Energy Review," Washington, DC, https://www.eia.gov/totalenergy/data/monthly/previous.php
[5] Freedonia Focus Reports, 2019, "Global Machine Tools." Cleveland, OH.
[6] Diaz, N., Helu, M., Jayanathan, S., Chen, Y., Horvath, A., and Dornfeld, D., 2010, "Environmental Analysis of Milling Machine Tool Use in Various Manufacturing Environments," Proceedings of the 2010 IEEE International Symposium on Sustainable Systems and Technology, ISSST 2010, Arlington, TX.
[7] Enparantza, R., Revilla, O., Azkarate, A., and Zendoia, J., 2006, "A Life Cycle Cost Calculation and Management System for Machine Tools," Proceedings of the 13th CIRP International Conference on Life Cycle Engineering, Leuven, Belgium.
[8] Kroll, L., Blau, P., Wabner, M., Frieß, U., Eulitz, J., and Klärner, M., 2011, "Lightweight Components for Energy-Efficient Machine Tools," CIRP J. Manuf. Sci. Technol., **4**(2), pp. 148–160.
[9] Herrmann, C., Dewulf, W., Hauschild, M., Kaluza, A., Kara, S., and Skerlos, S., 2018, "Life Cycle Engineering of Lightweight Structures," CIRP Ann., **67**(2), pp. 651–672.
[10] Helms, H., and Lambrecht, U. L., 2007, "The Potential Contribution of Light-Weighting to Reduce Transport Energy Consumption," Int. J. Life Cycle Assess., **12**(1), pp. 58–64.
[11] Yoon, H. S., Kim, E. S., Kim, M. S., Lee, J. Y., Lee, G. B., and Ahn, S. H., 2015, "Towards Greener Machine Tools—A Review on Energy Saving

Strategies and Technologies," Renewable Sustainable Energy Rev., **48**, pp. 870–891.
[12] Fortune Business Insights, 2020, "Vertical Milling Machine Market Size, Share and Industry Analysis, By Type (Turret Mills, Bed Mills, and Others), By Application (Automotive, General Machinery, Precision Engineering, Transport Machinery, and Others) and Regional Forecasts, 2019–2026," 2020, https://www.fortunebusinessinsights.com/vertical-milling-machine-market-102655
[13] Triebe, M. J., Mendis, G. P., Zhao, F., and Sutherland, J. W., 2018, "Understanding Energy Consumption in a Machine Tool Through Energy Mapping," Procedia CIRP, **69**, pp. 259–264.
[14] He, K., Tang, R., and Jin, M., 2017, "Pareto Fronts of Machining Parameters for Trade-off among Energy Consumption, Cutting Force and Processing Time," Int. J. Prod. Econ., **185**, pp. 113–127.
[15] Deb, K., Pratap, A., Agarwal, S., and Meyarivan, T., 2002, "A Fast and Elitist Multiobjective Genetic Algorithm: NSGA-II," IEEE Trans. Evol. Comput., **6**(2), pp. 182–197.
[16] Bian, J., Mohrbacher, H., Zhang, J. S., Zhao, Y. T., Lu, H. Z., and Dong, H., 2015, "Application Potential of High Performance Steels for Weight Reduction and Efficiency Increase in Commercial Vehicles," Adv. Manuf., **3**(1), pp. 27–36.
[17] Gokhale, A. A., Prasad, E. N., and Biswajit, B., 2019, "Light Weighting for Defense, Aerospace, and Transportation," *Indian Institute of Metals Series*, A. A. Gokhale, N. Eswara Prasad, and B. Basu, eds., Springer Singapore, Singapore.
[18] Broek, C. T., Singh, H., and Hillebrecht, M., 2012, "Lightweight Design for the Future Steel Vehicle," Auto Tech Rev., **1**(11), pp. 24–30.
[19] Hirsch, J., 2011, "Aluminium in Innovative Light-Weight Car Design," Mater. Trans., **52**(5), pp. 818–824.
[20] Tharumarajah, A., and Koltun, P., 2007, "Is There an Environmental Advantage of Using Magnesium Components for Light-Weighting Cars?," J. Cleaner Prod., **15**(11–12), pp. 1007–1013.
[21] Soutis, C., 2005, "Fibre Reinforced Composites in Aircraft Construction," Prog. Aerosp. Sci., **41**(2), pp. 143–151.
[22] Merklein, M., Johannes, M., Lechner, M., and Kuppert, A., 2014, "A Review on Tailored Blanks—Production, Applications and Evaluation," J. Mater. Process. Technol., **214**(2), pp. 151–164.
[23] Benjamin, L., and Wang, N., 2010, "The Boeing 787 Dreamliner Designing an Aircraft for the Future," J. Young Investig., **4026**, pp. 34–34.
[24] Möhring, H. C., 2017, "Composites in Production Machines," Procedia CIRP, **66**, pp. 2–9.
[25] Neugebauer, R., Wabner, M., Ihlenfeldt, S., Frieß, U., Schneider, F., and Schubert, F., 2012, "Bionics Based Energy Efficient Machine Tool Design," Procedia CIRP, **3**(1), pp. 561–566.
[26] Suh, J. D., Lee, D. G., and Kegg, R., 2002, "Composite Machine Tool Structures for High Speed Milling Machines," CIRP Ann., **51**(1), pp. 285–288.
[27] Sulitka, M., Novotny, L., Svéda, J., Strakos, P., Hudec, J., Smolik, J., and Vlach, P., 2008, "Machine Tool Lightweight Design and Advanced Control Techniques," Mod. Mach. Sci. J., pp. 29–33.
[28] Merlo, A., Ricciardi, D., Aggogeri, J., Meo, F., and Le Lay, L., 2008, "Application of Composite Materials for Lightweight and Smart Structures Design of High Performance Milling Machines," Proceedings of the 13th European Conference on Composite Materials, Stockholm, Sweden.
[29] Lv, J., Tang, R., Tang, W., Liu, Y., Zhang, Y., and Jia, S., 2017, "An Investigation Into Reducing the Spindle Acceleration Energy Consumption of Machine Tools," J. Cleaner Prod., **143**, pp. 794–803.
[30] Dietmair, A., Zulaika, J., Sulitka, M., Bustillo, A., and Verl, A., 2010, "Lifecycle Impact Reduction and Energy Savings Through Light Weight Eco-design of Machine Tools," Proceedings of the 17th CIRP Conference on Life Cycle Engineering, Anhui, China, pp. 105–110.
[31] Zulaika, J. J., Campa, F. J., N, L., and De Lacalle, L., 2011, "An Integrated Process–Machine Approach for Designing Productive and Lightweight Milling Machines," Int. J. Mach. Tools Manuf., **51**(7–8), pp. 591–604.
[32] Li, B., Hong, J., and Liu, Z., 2014, "Stiffness Design of Machine Tool Structures by a Biologically Inspired Topology Optimization Method," Int. J. Mach. Tools Manuf., **84**, pp. 33–44.
[33] Zhao, L., Chen, W.-Y., Ma, J.-F., and Yang, Y.-B., 2008, "Structural Bionic Design and Experimental Verification of a Machine Tool Column," J. Bionic Eng., **5**, pp. 46–52.
[34] Zhao, L., Ma, J., Wang, T., and Xing, D., 2010, "Lightweight Design of Mechanical Structures Based on Structural Bionic Methodology," J. Bionic Eng., **7**(4), pp. S224–S231.
[35] Triebe, M. J., Zhao, F., and Sutherland, J. W., 2019, "Achieving Energy Efficient Machine Tools by Mass Reduction Through Multi-objective Optimization," Procedia CIRP, **80**, pp. 73–78.
[36] Li, B., Hong, J., Wang, Z., Wu, W., and Chen, Y., 2012, "Optimal Design of Machine Tool Bed by Load Bearing Topology Identification With Weight Distribution Criterion," Procedia CIRP, **3**(1), pp. 626–631.
[37] Saidur, R., 2010, "A Review on Electrical Motors Energy Use and Energy Savings," Renewable Sustainable Energy Rev., **14**(3), pp. 877–898.
[38] Capehart, B. L., Turner, W. C., and Kennedy, W. J., 2006, *Guide to Energy Management*, 5th ed., Fairmont Press; Distributed by CRC/Taylor & Francis, Lilburn, GA : Boca Raton, FL.